

Q Can you list all the properties of the carrier-smoothing filter?

GNSS Solutions is a regular column featuring questions and answers about technical aspects of GNSS. Readers are invited to send their questions to the columnist, **Dr. Mark Petovello**, Department of Geomatics Engineering, University of Calgary, who will find experts to answer them. His e-mail address can be found with his biography below.

Carrier-smoothing filters, also known as Hatch filters, are commonly used to reduce (“smooth”) the noise and multipath errors in pseudorange measurements by exploiting the high-precision relative distance information from carrier phase measurements. However, carrier-smoothing filters operate on more than just noise and multipath, and this article summarizes the response of such filters to all relevant inputs.

The GNSS carrier-smoothing filter is governed by the following finite difference equation

$$r_{sm}[n] = \frac{M-1}{M} r_{sm}[n-1] + \frac{1}{M} r_c[n] + \frac{M-1}{M} (r_p[n] - r_p[n-1]) \quad (1)$$

for $n > 0$ where $r_{sm}[n]$ is the filter output at the n -th epoch, whereas $r_c[n]$ and $r_p[n]$ are the code and phase pseudoranges, respectively. For the initial condition when $n = 0$, $r_{sm}[n] = r_c[n]$.

In this article we will analyze the case in which parameter M , which relates to the bandwidth of the filter (larger M gives more smoothing), is constant. **Figure 1** shows a block diagram of the carrier-smoothing system. We use the following fundamental signals: the impulse signal $\delta[n] = 1$ for $n = 0$ and

0 for $n \neq 0$, and the step signal $u[n] = 1$ for $n \geq 0$ and 0 for $n < 0$. The output of the block with transfer function z^{-1} is $x[n-1]$ when the input is $x[n]$.

Taking into account the main errors, the code pseudorange can be written as

$$r_c[n] = r[n] + c_s[n] + c_R[n] + T[n] + I[n] + w_c[n] \quad (2)$$

where $r[n]$ is the true range between the satellite and the GNSS receiver, $c_s[n]$ is the error due to the bias of the satellite clock, $c_R[n]$ is the error due to the bias of the receiver clock, $T[n]$ is the error due to the troposphere delay, $I[n]$ is the error due to the ionosphere delay, $w_c[n]$ is the noise due to the receiver DLL (delay locked loop) jitter due to thermal noise and noise-like multipath. All the quantities are measured in meters.

The phase pseudorange can be written as

$$r_p[n] = r[n] + c_s[n] + c_R[n] + T[n] - I[n] + N[n]\lambda + w_p[n] \quad (3)$$

where $N[n]$ is the integer ambiguity, λ is the wavelength, and $w_p[n]$ is the noise due to the receiver PLL (phase locked loop) jitter plus the effect of multipath. The integer ambiguity should be constant $N[n] = N_0$ during the satellite visibility, but we consider here that cycle slips may occur and therefore the integer ambiguity becomes a time-varying signal.

In general, the product of the carrier wavelength and the integer ambiguity, $\lambda N[n]$, can be written as

$$\lambda N[n] = \lambda N_0 + \sum_{k=0}^{N_{c.s.}-1} \lambda d_k u[n - n_k] \quad (4)$$

where $n_k > 0$ is the discrete-time at which the k -th cycle slip event occurs, d_k the number of cycles in the slip (integer, positive or negative), $N_{c.s.}$ is the number of cycle slip events in the observation time. Parameter N_0 is the value of $N[n]$ at $n = 0$, which can be set equal to zero, since it cancels out in (1) for $n > 0$.

Both pseudoranges have a common term $s[n] = r[n] + c_s[n] + c_R[n] + T[n]$. They also have the term $I[n]$ with opposite sign, and each one has its own noise component ($w_p[n]$ and $w_c[n]$), which are statistically independent.

In the following sections, we analyze the outputs of the carrier-smoothing system when one and only one of the various components is present. The total system output is then given by the sum of all the individual outputs, thanks to the system's linearity.



MARK PETOVELLO is a Professor in the Department of Geomatics Engineering at the University of Calgary. He has been actively involved in many aspects of positioning and navigation since 1997 including GNSS algorithm development, inertial navigation, sensor integration, and software development. Email: mark.petovello@ucalgary.ca

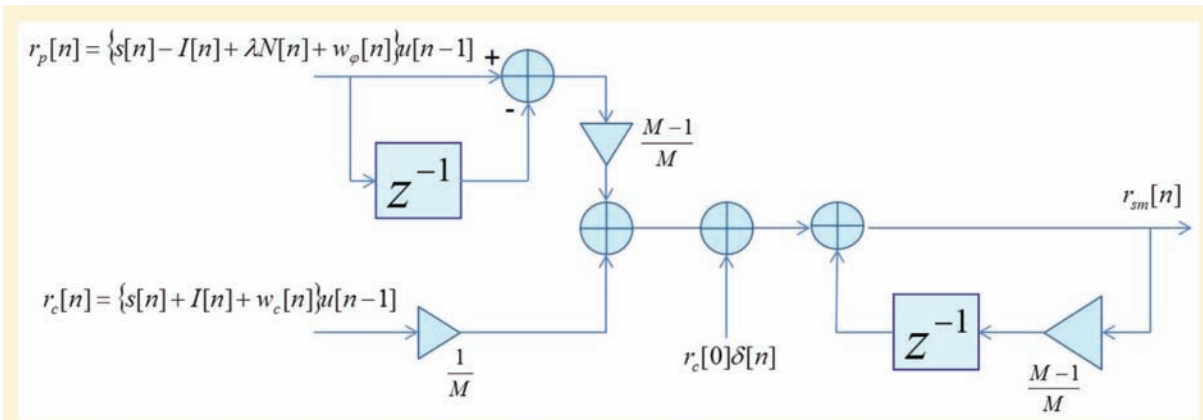


FIGURE 1 Block diagram of the carrier-smoothing system

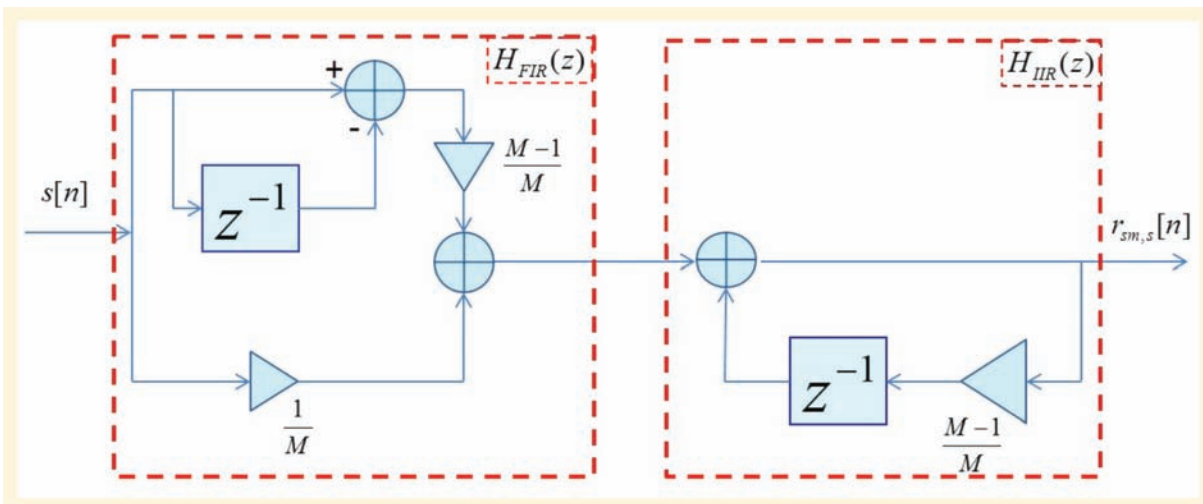


FIGURE 2 Block diagram of the carrier-smoothing system for the common component $s[n]$

Tables 1–3 list all the relevant formulas and figures. Transfer functions are identified as $H_x(z)$ (z complex number), impulse responses as $h_x[n]$ (n integer), step responses as $u_x[n]$ where x specifies the considered component. In the tables, $H_x(f)$ is defined as $H_x(f) = H_x(e^{j2\pi f})$ where f is the normalized frequency; the true frequency is $f' = f/T$ (in hertz) where T is the time interval between two subsequent epochs.

Common Component

For the common signal $s[n]$, the system has just one input and one output, as shown in Figure 2. In this case we can evaluate the transfer function in the z -domain, as the cascade of two subsystems. The first subsystem is a finite impulse response (FIR) filter with transfer function:

$$H_{FIR}(z) = \frac{1}{M} + \frac{M-1}{M} - \frac{M-1}{M} z^{-1} = 1 - \frac{M-1}{M} z^{-1}; \quad (5)$$

The second subsystem is instead an infinite impulse response (IIR) filter with the following transfer function

$$H_{IIR}(z) = \frac{1}{1 - \frac{M-1}{M} z^{-1}} = \frac{z}{z - \frac{M-1}{M}} \quad (6)$$

and thus, the transfer function and impulse response of the entire system with input $s[n]$ are, respectively,

$$H_s(z) = H_{FIR}(z)H_{IIR}(z) = 1, \quad h_s[n] = \delta[n] \quad (7)$$

as also reported in (20) and (21) of Table 1. Thus, we have $r_{sm,s}[n] = s[n] * h_s[n] = s[n]$, which means that the true range, the troposphere delay, and the terms due to the clock bias are present without alterations at the output of the filter.

Initial Condition

The initial condition can be interpreted as an impulse $r_c[0] \delta[n]$ which enters the low-pass IIR filter and provides the output $r_{sm,i.c.}[n] = r_c[0]h_{i.c.}[n]$, where $h_{i.c.}[n]$ and its plots for $M=30$ and 100 are reported in Table 2: equation (28) and the figure at its right. We can see that a long transient exists, which has theoretically an infinite duration but can be quantified

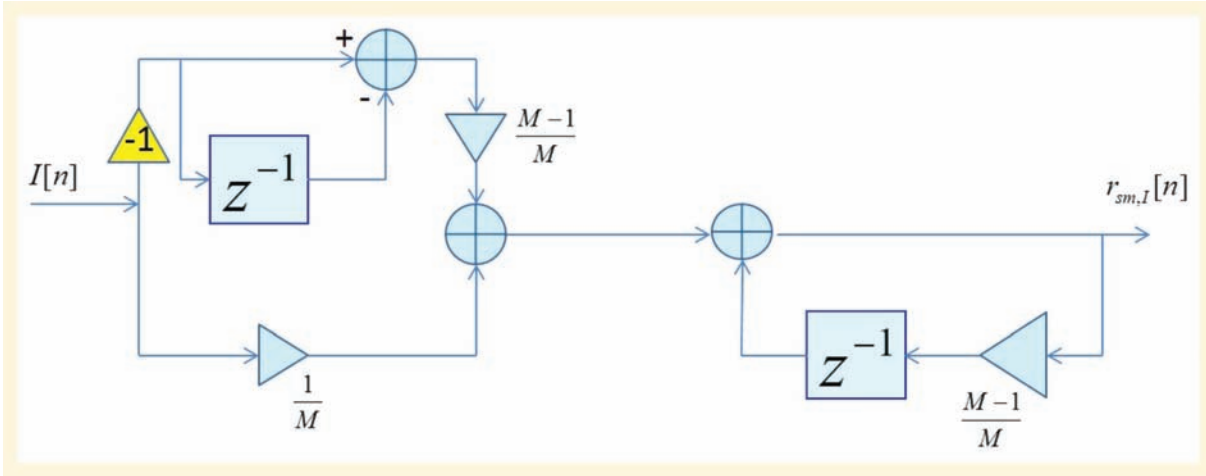


FIGURE 3 Block diagram of the carrier-smoothing system for the ionosphere component

through the partial energy $E_{i.c.}[n]$. It is possible to show that

$$E_{i.c.}[n] = \sum_{k=-\infty}^{n-1} (h_{i.c.}[k])^2 = \left[1 - \left(\frac{M-1}{M} \right)^{2n} \right] E_{i.c.} \quad (8)$$

with $E_{i.c.}$ being the total energy of $h_{i.c.}[n]$ for $n \rightarrow \infty$. The impulse response reaches 98 percent of its total energy after approximately $2M$ samples. We can therefore state that, according to the 98 percent criterion, the transient ends at the discrete time $2M$.

Cycle Slip

Let us consider the effects of just one cycle slip event, i.e., $\lambda N[n] = \lambda d_0 u[n - n_0]$ in (4). The transfer function $H_{c.s.}(z)$ of the system with input $\lambda N[n]$ and output $r_{sm,c.s.}[n]$ is given in (29) of Table 2. The response to $\lambda d_0 u[n - n_0]$ is the inverse z-transform of $R_{sm,c.s.}(z) = H_{c.s.}(z) \lambda d_0 z^{-n_0} / (1 - z^{-1})$:

$$r_{sm,c.s.}[n] = \lambda d_0 \frac{M-1}{M} \left(\frac{M-1}{M} \right)^{n-n_0} u[n-n_0] \quad (9)$$

The figure on the right of (31) in Table 2 shows the step response for $M=30$ and 100 : as M increases, the coefficient gets closer to 1, and the duration of $r_{sm,c.s.}[n]$ increases. Using the 98 percent criterion, the transient is over $2M$ samples after the occurrence of the cycle slip.

Ionosphere Component

The analysis of the ionosphere component can be performed using the block diagram of Figure 3. In this case, the first filter has transfer function

$$H_{FIR,iono}(z) = \frac{1}{M} - \frac{M-1}{M} + \frac{M-1}{M} z^{-1} = \frac{2-M}{M} + \frac{M-1}{M} z^{-1} \quad (10)$$

while the second filter is again the same IIR filter of Figure 2 described by equation (6).

Therefore, the transfer function for the ionosphere component $I[n]$ is $H_{iono}(z) = H_{FIR,iono}(z) H_{IIR}(z)$, given in (22) of Table 1. Equation (25) in Table 1 gives the corresponding impulse response $h_{iono}[n]$, with plots for $M=30$ and 100 on its right.

Then the carrier-smoothing filter output due to the ionosphere can be written as

$$r_{sm,I}[n] = I[n] * h_{iono}[n] \quad (11)$$

which unfortunately does not provide much information; so, some approximations are necessary. Filter $H_{iono}(z)$ has a zero, $(M-1)/(M-2)$, and a pole, $(M-1)/M$, very close to each other. The system then tends to behave as an all-pass filter, as shown in the figure on the right of (23) in Table 1, where the modulus of the transfer function $\mathbf{H}_{iono}(f) = H_{iono}(\exp(j2\pi f))$ is plotted versus the normalized frequency f . The group delay of the system is defined as

$$\theta_{iono}(f) \stackrel{\text{def}}{=} -\frac{1}{2\pi} \frac{d\varphi_{iono}(f)}{df} \quad (12)$$

where $\varphi_{iono}(f)$ is the phase of $\mathbf{H}_{iono}(f)$, shown in the figure on the right of (24) in Table 1. We can show that, for small values of f ,

$$\theta_{iono}(f) \approx -\frac{(a-b)[(1-a)(1-b) + (2\pi f)^2] - (a-b)8\pi^2 f^2}{[(1-a)(1-b) + (2\pi f)^2]^2} \quad (13)$$

having defined $a=(M-1)/(M-2)$ and $b=(M-1)/M$.

In nominal conditions, the ionosphere component $I[n]$ changes slowly, which means that its bandwidth is very small, and we can approximate the transfer function in the frequency domain as

$$\mathbf{H}_{iono}(f) \approx M_{iono} \exp[-j2\pi\tau_i f]$$

where $M_{iono} = 1$ is the magnitude of $\mathbf{H}_{iono}(f)$ at $f = 0$, and τ_i is the group delay $\theta_{iono}(f)$ at $f = 0$:

$$\theta_{iono}(0) \approx -\frac{(a-b)(1-a)(1-b)}{[(1-a)(1-b)]^2} = \frac{b-a}{(1-a)(1-b)} = 2(M-1) \quad (14)$$

Then, for a sufficiently slow ionosphere component $I[n]$, the output of the carrier-smoothing filter is approximately equal to $r_{sm,I}[n] \approx I[n - 2(M-1)]$ with a delay $\tau_i = 2(M-1)$, which decreases as M decreases.

Noise Components

A discrete-time white Gaussian noise process $w_{in}[n]$, with

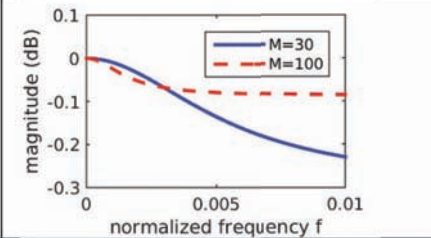
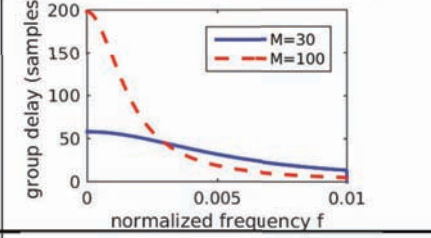
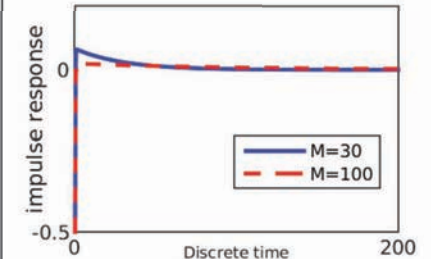
Common component $s[n]$	$H_s(z) = 1, H_s(f) = 1$	(20)	
	$h_s[n] = \delta[n]$	(21)	
Ionosphere contribution $I[n]$	$H_{iono}(z) = -\frac{M-2}{M} \frac{z - \frac{M-1}{M}}{z - \frac{M-1}{M}}$	(22)	
	$ H_{iono}(f) ^2 = H_{iono}(z) ^2 \Big _{z=\exp(j2\pi f)}$	(23)	
	$\theta_{iono}(f)$	(24)	
	$h_{iono}[n] = -\frac{M-2}{M} \delta[n] + \frac{2}{M} \left(\frac{M-1}{M}\right)^n u[n-1]$	(25)	

TABLE 1. Summary of the theoretical results for the common component $s[n]$ and the ionosphere contribution $I[n]$ at the output of the smoothing filter; the plots consider the two cases $M=30$ and 100 .

zero mean and variance σ_w^2 which enters a filter with impulse response $h[n]$, generates an output process $w_{out}[n]$ that is no longer white, but still Gaussian, with zero mean and with variance

$$\sigma_{out}^2 = \sigma_w^2 \sum_{j=-\infty}^{\infty} h^2[j] \quad (15)$$

Code Pseudorange Noise. Code pseudorange noise generates an output process $r_{sm,c,n}[n]$ which is obtained by using $w_c[n]$ as input of the filter with impulse response $h_c[n] = h_{IR}[n]/M$. Using (15) and the total energy (obtained from (8) for $n \rightarrow \infty$) we get the output variance $\sigma_{c,out}^2$:

$$\sigma_{c,out}^2 = \sigma_c^2 \sum_{j=-\infty}^{\infty} h_c^2[j] = \frac{\sigma_c^2}{2M-1} \quad (16)$$

where σ_c^2 is the variance of $w_c[n]$. The figure on the right of (32) in Table 3 shows how $\sigma_{c,out}^2$ decreases to zero as M increases. This is the “smoothing” aspect of the filter.

Phase Pseudorange Noise. Phase pseudorange noise generates an output process $r_{sm,p,n}[n]$ which is obtained by using $w_p[n]$ as input of the filter with impulse response $h_p[n] = (M-1)\{h_{IR}[n] - h_{IR}[n-1]\}/M$, which can be written as follows:

$$h_p[n] = \frac{M-1}{M} \delta[n] - \frac{1}{M} \left(\frac{M-1}{M}\right)^n u[n-1]$$

The exact variance $\sigma_{p,out}^2$ of $r_{sm,p,n}[n]$ is

$$\sigma_{p,out}^2 = \sigma_p^2 \sum_{n=-\infty}^{\infty} h_p^2[n] = \sigma_p^2 \left(\frac{M-1}{M}\right)^2 \frac{2M}{2M-1} \quad (17)$$

where σ_p^2 is the variance of $w_p[n]$. The figure on the right of (33) in Table 3 shows how $\sigma_{p,out}^2$ increases with M with an asymptotic value equal to σ_p^2 which means that the system tends to behave as an all-pass filter as M increases (although since σ_p is typically much smaller than σ_c , this is not a major concern).

Summary of the Results

In the presence of all the errors, the signal at the output of the carrier-smoothing filter is then

$$r_{sm}[n] = s[n] + r_{sm,i,c}[n] + r_{sm,c,s}[n] + r_{sm,c,n}[n] + r_{sm,p,n}[n] + r_{sm,l}[n] \quad (18)$$

Table 1 lists the results valid for the common and ionosphere components $s[n]$ and $I[n]$. Table 2 refers to effects due to the initial condition and the cycle slips. Table 3 summa-

Initial condition contribution	$H_{i.c.}(z) = \frac{z}{z - \left(\frac{M-1}{M}\right)} \quad (26)$	
	$ H_{i.c.}(f) ^2 = H_i(z) ^2 \Big _{z=\exp(j2\pi f)} \quad (27)$	
	$h_{i.c.}[n] = \left(\frac{M-1}{M}\right)^n u[n] \quad (28)$	
Cycle slip contribution	$H_{c.s.}(z) = \frac{M-1}{M} \frac{z-1}{z - \left(\frac{M-1}{M}\right)} \quad (29)$	
	$ H_{c.s.}(f) ^2 = H_N(z) ^2 \Big _{z=\exp(j2\pi f)} \quad (30)$	
	$u_{c.s.}[n] = \left(\frac{M-1}{M}\right)^{n+1} u[n] \quad (31)$	

TABLE 2 Summary of the theoretical results for the initial condition $rc[0]\delta[n]$ and the variation of the integer ambiguity $N[n]$ at the output of the smoothing filter; the plots consider the two cases $M=30$ and 100 .

rizes the results obtained for the noise and multipath inputs $w_c[n]$ and $w_p[n]$.

On the one hand, we see that larger values of M decrease the output noise variance due to code pseudorange, but on the other hand these larger values increase the duration of transients in the presence of cycle slips; so, a compromise must be found. The total noise variance at the output of the carrier-smoothing filter is

$$\sigma_{c,out}^2 + \sigma_{p,out}^2 = \frac{\sigma_c^2}{2M-1} + \sigma_p^2 \left(\frac{M-1}{M}\right)^2 \frac{2M}{2M-1} \approx \frac{\sigma_c^2}{2M-1} + \sigma_p^2 \quad (19)$$

and cannot decrease below the value σ_p^2 even if M tends to infinity. Then, one criterion to set the value of parameter M is to make the variances of two noise components equal:

$$\frac{\sigma_c^2}{2M-1} \approx \sigma_p^2 \Rightarrow (2M-1) \approx \frac{\sigma_c^2}{\sigma_p^2} \Rightarrow M \approx \frac{\sigma_c^2}{2\sigma_p^2}$$

With this value of M , the noise variance at the output of the smoothing filter is equal to $2\sigma_p^2$ and the transient durations are reasonably short. However, if cycle slips are frequent, then transients are the dominating error and M should be chosen, taking into consideration the probability and magnitude of undetectable cycle slips.

Authors

LETIZIA LO PRESTI is a full professor of signal theory and statistical signal processing at Politecnico di Torino, Italy. Her research covers the field of digital signal processing, simulation of communication systems, array processing for adaptive antennas, and the technology of navigation and positioning systems,

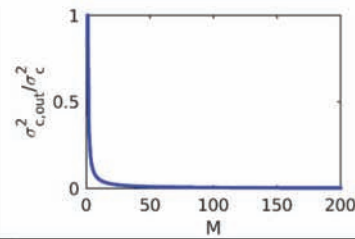
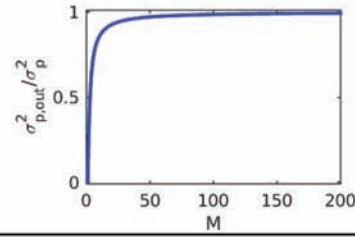
Code noise variance	$\sigma_{c,out}^2 = \frac{\sigma_c^2}{2M-1} \quad (32)$	
Phase noise variance	$\sigma_{p,out}^2 = \sigma_p^2 \left(\frac{M-1}{M} \right)^2 \frac{2M}{2M-1} \quad (33)$	
Overall output noise variance	$\sigma_{c,out}^2 + \sigma_{p,out}^2 = \frac{\sigma_c^2}{2M-1} + \sigma_p^2 \left(\frac{M-1}{M} \right)^2 \frac{2M}{2M-1} \quad (34)$	

TABLE 3. Summary of the theoretical results for the noise terms at the output of the smoothing filter



with focus on GNSS receivers. She is the head of the NavSAS group, focused on research activities in the field of global navigation satellite systems, and since 2003 she has been the scientific coordinator of

the Master on Navigation and Related Applications held by Politecnico di Torino.

MONICA VISINTIN is an associate professor of signal theory and digital communications at Politecnico di Torino. She received her master of science degree in electrical engineering from the University of California at Los Angeles (UCLA) and



the Ph.D. degree in electronic engineering from Politecnico di Torino. Her main research activities are in the field of satellite and optical communications. She is a member of IEEE.



THE COMPLETE COMPACT INS PACKAGE

ReACT-INS

GNSS-Inertial Compact Antenna with Processor

Choice of Commercial and P-Code GNSS Receivers

RTK Capable GNSS Solution

Precision Roll, Pitch and Heading

5G and 300 Deg/Sec Performance

Fixed Lever Arms for Easy Installation

Dual Antenna Heading Stabilisation Option





UK: +44-1524-383320 | DE: +49-9367-9878-080 | www.forsbergservices.co.uk

